

Synthesis and Reactivity of *N*-Heterocycle-B(C₆F₅)₃ Complexes. 4. Competition between Pyridine- and Pyrrole-Type Substrates toward B(C₆F₅)₃: Structure and Dynamics of 7-B(C₆F₅)₃-7-azaindole and [7-Azaindolum]⁺[HOB(C₆F₅)₃]⁻

Francesca Focante,^{*,†,‡} Isabella Camurati,[#] Luigi Resconi,[#] Simona Guidotti,[#] Tiziana Beringhelli,^{*,‡}
Giuseppe D'Alfonso,[‡] Daniela Donghi,[‡] Daniela Maggioni,[‡] Pierluigi Mercandelli,^{*,§} and Angelo Sironi[§]

Dipartimento di Chimica Organica "A. Mangini", Università di Bologna, Viale Risorgimento 4, I-40136 Bologna, Italy, Basell Polyolefins Italia, Centro Ricerche "G. Natta", I-44100 Ferrara, Italy, Dipartimento di Chimica Inorganica, Metallorganica e Analitica, Facoltà di Farmacia, Università degli Studi di Milano, Via Venezian 21, I-20133 Milano, Italy, and Dipartimento di Chimica Strutturale e Stereochimica Inorganica, Università degli Studi di Milano, Via Venezian 21, I-20133 Milano, Italy

Received July 29, 2005

Reaction between 7-azaindole and B(C₆F₅)₃ quantitatively yields 7-(C₆F₅)₃B-7-azaindole (**4**), in which B(C₆F₅)₃ coordinates to the pyridine nitrogen of 7-azaindole, leaving the pyrrole ring unreacted even in the presence of a second equivalent of B(C₆F₅)₃. Reaction of 7-azaindole with H₂O–B(C₆F₅)₃ initially produces [7-azaindolum]⁺[HOB(C₆F₅)₃]⁻ (**5**) which slowly converts to **4** releasing a H₂O molecule. Pyridine removes the borane from the known complexes (C₆F₅)₃B-pyrrole (**1**) and (C₆F₅)₃B-indole (**2**), with formation of free pyrrole or indole, giving the more stable adduct (C₆F₅)₃B-pyridine (**3**). The competition between pyridine and 7-azaindole for the coordination with B(C₆F₅)₃ again yields **3**. The molecular structures of compounds **4** and **5** have been determined both in the solid state and in solution and compared to the structures of other (C₆F₅)₃B-*N*-heterocycle complexes. Two dynamic processes have been found in compound **4**. Their activation parameters ($\Delta H^\ddagger = 66$ (3) kJ/mol, $\Delta S^\ddagger = -18$ (10) J/mol K and $\Delta H^\ddagger = 76$ (5) kJ/mol, $\Delta S^\ddagger = -5$ (18) J/mol K) are comparable with those of other (C₆F₅)₃B-based adducts. The nature of the intramolecular interactions that result in such energetic barriers is discussed.

Introduction

Pyridine undergoes a range of simple electrophilic additions involving donation of the nitrogen lone pair to an electrophile and subsequent generation of the pyridinium salt, which maintains the aromatic sextet.^{1,2} In particular, the reaction with the strong Lewis acid tris(pentafluorophenyl)borane, B(C₆F₅)₃, yields the stable adduct (C₆F₅)₃B-NC₅H₅ (**3**).^{3,4}

B(C₆F₅)₃, in general, shows a very strong affinity as a Lewis acid for different nitrogen functionalities such as amines, imines, nitriles, and aromatic *N*-heterocycles.^{5,6} Pyrroles and indoles usually do not react with electrophiles at the nitrogen position because of the lack of the basic lone pair, which is engaged in the aromatic π -system; however, when pyrrole and indole are reacted with B(C₆F₅)₃, instantaneous and quantitative formation of 1:1 B–N adducts takes place ((C₆F₅)₃B-5*H*-pyrrole, **1**; (C₆F₅)₃B-3*H*-indole, **2**), likely resulting from the previous protonation of the pyrrole double bond by a catalytic amount of H₂O–B(C₆F₅)₃ and the subsequent reaction at the newly formed iminic nitrogen.⁷ This reaction is shown in Scheme 1.

* To whom correspondence should be addressed. E-mail: francesca.focante@basell.com (F.F.); tiziana.beringhelli@unimi.it (T.B.); pierluigi.mercandelli@unimi.it (P.M.).

[†] Dipartimento di Chimica Organica "A. Mangini", Università di Bologna.

[#] Basell Polyolefins Italia, Centro Ricerche "G. Natta".

[‡] Dipartimento di Chimica Inorganica, Metallorganica e Analitica, Facoltà di Farmacia, Università degli Studi di Milano.

[§] Dipartimento di Chimica Strutturale e Stereochimica Inorganica, Università degli Studi di Milano.

(1) Joule, J. A.; Mills, K. *Heterocyclic Chemistry*, IV ed.; Blackwell: London, 2000; Chapter 5.

(2) Wilson, J. W.; Worrall, I. J. *Inorg. Nucl. Chem. Lett.* **1967**, 3, 57.

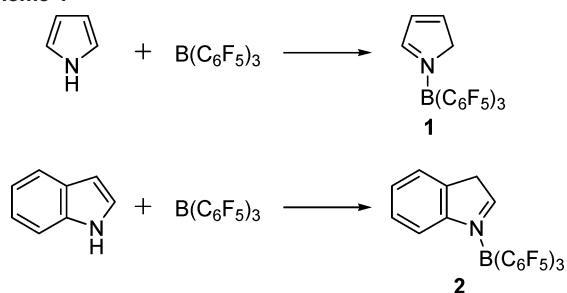
(3) Massey, A. G.; Park, A. J. *J. Organomet. Chem.* **1964**, 2, 245.

(4) Holtcamp M. W. Int. Patent Application WO 99/64476.

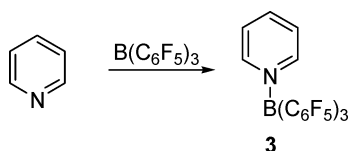
(5) Piers, W. E. *Adv. Organomet. Chem.* **2005**, 52, 1 and references therein.

(6) Focante, F.; Mercandelli, P.; Sironi, A.; Resconi, L. *Coord. Chem. Rev.* **2005**, in press and references therein.

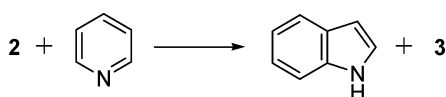
Scheme 1



Scheme 2



Scheme 3



As part of our study of the structural and dynamic features and reactivity of $(\text{C}_6\text{F}_5)_3\text{B-N}$ -heterocycle complexes, in this paper, we compare (i) the different reactivities of $\text{B}(\text{C}_6\text{F}_5)_3$ toward pyridine- and pyrrole/indole-type substrates since both heterocycles lead to stable adducts with a B–N bond and (ii) the dynamic processes in these compounds.

Results and Discussion

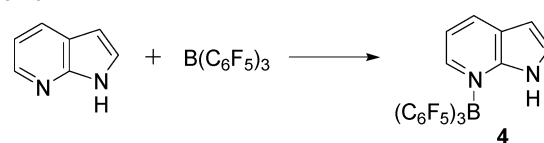
1. Synthesis and Reactivity. Pyridine, when treated with 1 equiv of $\text{B}(\text{C}_6\text{F}_5)_3$, instantaneously and quantitatively gives the Lewis acid–base adduct **3** (Scheme 2).^{3,4}

When adducts **1** or **2** are treated with pyridine, pyrrole and indole, respectively, are freed, and complex **3** is formed immediately and quantitatively (Scheme 3, reaction exemplified for complex **2**). The mechanism probably follows a dissociative path, analogous to that of the exchange reactions occurring with other $\text{B}(\text{C}_6\text{F}_5)_3$ complexes.^{5,6,8}

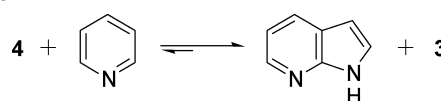
The driving force for the reaction shown in Scheme 3 is the recovery of aromaticity in the five-membered ring of indole (or pyrrole), while, in the case of pyridine, the coordination reaction with $\text{B}(\text{C}_6\text{F}_5)_3$ does not alter the resonance stabilization in the six-membered ring. Therefore borane strongly prefers coordination to the nitrogen of pyridine, and this can be directly observed in the reaction of $\text{B}(\text{C}_6\text{F}_5)_3$ with 7-azaindole, where $\text{B}(\text{C}_6\text{F}_5)_3$ coordinates exclusively to the pyridinic moiety of the molecule (Scheme 4).

In addition, it has been observed that coordination of $\text{B}(\text{C}_6\text{F}_5)_3$ to pyridine is favored with respect to coordination with 7-azaindole, in fact the pyridine displaces the latter from complex **4** to give the pyridine complex **3** (Scheme 5). This

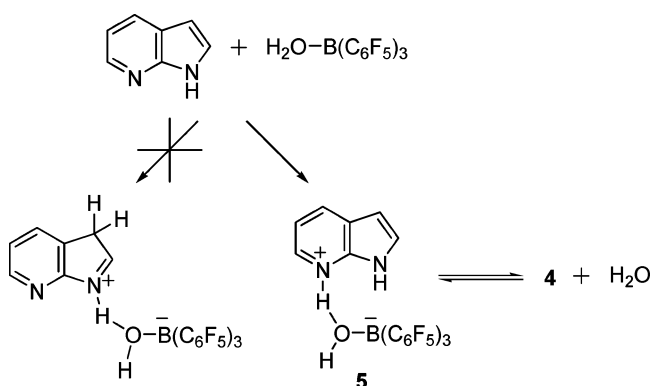
Scheme 4



Scheme 5



Scheme 6



behavior can be explained by taking into account the stronger basicity of pyridine ($\text{p}K_{\text{a}} = 5.25$) with respect to 7-azaindole ($\text{p}K_{\text{a}} = 4.59$).⁹ The reaction however is not instantaneous like the one with complex **2**, but it takes several days. A kinetic study performed on two samples of **4** in CD_2Cl_2 treated with 1 and 5 equiv of pyridine showed that the rate of disappearance of **4** is independent of the pyridine concentration, indicating that the exchange reaction occurs through a dissociative mechanism ($t_{1/2} = 15.2$ h, see Figure S1 in Supporting Information) according to literature data for analogous compounds.^{5,6,8}

Attempts to react **4** with a second equivalent of $\text{B}(\text{C}_6\text{F}_5)_3$ to obtain a diborane complex failed, likely because of both steric and electronic reasons. In fact, the presence of a positively charged nitrogen, from the coordination with boron, inductively affects the nucleophilicity of the five-membered ring. For example, the reaction of **4** with the strong Brønsted acid $\text{H}_2\text{O}-\text{B}(\text{C}_6\text{F}_5)_3$,⁸ aimed at protonating the pyrrolic ring in the β -position, does not take place. On the other hand, the 1:1 reaction of 7-azaindole with $\text{H}_2\text{O}-\text{B}(\text{C}_6\text{F}_5)_3$ produces the azaindolum salt **5**, which slowly displaces the H_2O molecule to form complex **4**, while no protonation of the pyrrole double bond is observed (Scheme 6).¹⁰ The experiment was carried out in deuterated dichloromethane and monitored at different times with ^1H NMR analyses. Spectra showed instantaneous formation of salt **5** and slow conversion into **4** (67% in 24 h); the reaction did not evolve further with time.¹¹

Complex **5** is however quite stable in the solid state: a mixture of **4** and **5** in toluene solution and a solution of **4** in

(7) Guidotti, S.; Camurati, I.; Focante, F.; Angellini, L.; Moscardi, G.; Resconi, L.; Leardini, R.; Nanni, D.; Mercandelli, P.; Sironi, A.; Beringhelli, T.; Maggioni, D. *J. Org. Chem.* **2003**, *68*, 5445.

(8) Bergquist, C.; Bridgewater, B. M.; Harlan, C. J.; Norton, J. R.; Friesner, R. A.; Parkin, G. *J. Am. Chem. Soc.* **2000**, *122*, 10581.

(9) Adler, T. K.; Albert, A. *J. Chem. Soc.* **1960**, 1794.

(10) Indole can be easily protonated at its C-3 with formation of the 3H-indolum cation, see: Joule, J. A.; Mills, K. *Heterocyclic Chemistry*, IV ed.; Blackwell: London, 2000; Chapter 16.

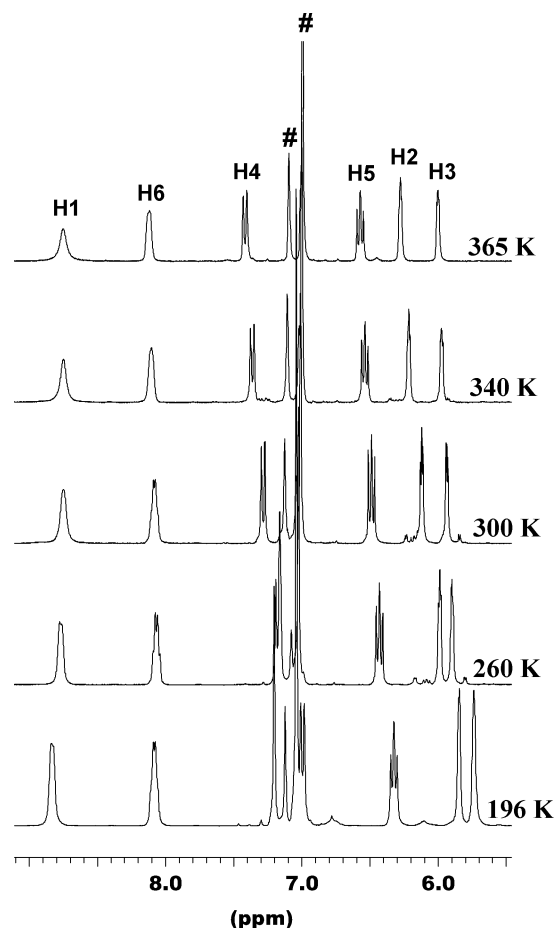


Figure 1. Variable-temperature ¹H NMR spectra of **4** (7.1 T, # marks toluene). The resonances are labeled according to Figure 3.

nonanhydrous toluene, both kept at $-5\text{ }^{\circ}\text{C}$ for a few days, gave colorless crystals of **5** suitable for X-ray single-crystal analysis. Crystals of compound **4** were obtained from anhydrous dichloromethane by cooling the solution for several months at $-25\text{ }^{\circ}\text{C}$.

2. Solution Structure of Adducts 4 and 5. The ¹H NMR spectrum of adduct **4** in toluene-*d*₈ (Figure 1) shows, at 300 K, six signals that have been assigned by 2D scalar and dipolar correlation experiments (see Figures S2–S4). When the temperature is lowered, the resonances shifted to high field, eventually leading to the inversion of H2 and H3. In contrast, below 260 K, the two lower field signals (H1 and H6) shift to lower fields. These shifts, together with the shape itself of these signals, suggest the occurrence of intramolecular N–H···F and C–H···F “through-space” couplings. Indeed a {¹⁹F}¹H spectrum recorded at 233 K (Figure S5) shows that, upon fluorine decoupling, the H1 pseudo-doublet becomes a singlet, and the H6 quartet becomes a doublet.

In the ¹⁹F spectrum at 300 K, the appearance of fifteen resonances indicates conformational rigidity on the NMR time scale (*C*₁ symmetry). When the temperature was increased (Figure 2), a generalized broadening of the signals

(11) Small amounts of compound **5** can also be observed in the solution of **4** because of the reaction with adventitious water present in the solvents. The relative amount of the two species remains constant with time, and no decomposition reactions leading to borane cleavage are observed for weeks.

Table 1. Assignments of the ¹⁹F Resonances of Compound **4** at 233 K (δ)

ring	ortho	para	meta
A	–127.22 (A2)	–153.95 (A4)	–160.86 (A5)
	–131.37 (A6)		–162.26 (A3)
B	–127.57 (B2)	–154.95 (B4)	–161.99 (B3)
	–137.46 (B6)		–162.30 (B5)
C	–131.64 (C2)	–153.78 (C4)	–162.10 (C3)
	–134.94 (C6)		–163.07 (C5)

Table 2. Dipolar and Scalar Correlation Observed between the Resonances of Adduct **4**

¹⁹ F– ¹⁹ F COSY	¹ H– ¹⁹ F COSY	¹⁹ F– ¹⁹ F NOESY	¹ H– ¹⁹ F HOESY
A2–B6	H6–A2	A2–B6	H6–A2
B2–A6	H6–C2	A6–B2	H6–C2
B2–C6	H1–C6	C6–B2	H1–C6
		A6–C2	H1–B6

occurred showing the onset of dynamic processes responsible for the loss of the H···F couplings in the corresponding proton spectra.

To establish the solution structure of **4**, first the ¹⁹F resonances of the three aryl rings (Table 1) have been assigned by means of [¹⁹F–¹⁹F] COSY (Figure S6) performed at 233 K; then, the relative orientations of the three rings and of the heterocyclic moiety have been established on the basis of the ¹⁹F–¹H and ¹⁹F–¹⁹F dipolar interactions, (Figure S7 and Figure S8) and of the ortho ¹⁹F–¹⁹F through-space scalar correlations (Figure S9).

Shortly, four short H···F distances and four short interring distances, F···F, characterize the solution structure of the adduct **4**. Table 2 reports the pairs of signals between which homo- and heteronuclear nOe’s, as well as “through-space” scalar correlations, have been observed. The solution structure derived accordingly is shown in Figure 3 and is substantially identical to the one determined in the solid state (see below). The plane of B ring is almost coplanar with the N–B bond and can be regarded as the *in-plane* substituent in the complex conformation,¹² while the other two adopt a two-bladed propellerlike conformation.

As far as adduct **5** is concerned, even at 183 K the ¹⁹F NMR spectrum in toluene-*d*₈ shows only three signals, indicating that the ion-pair interaction is not tight enough to stop the free rotation of the three aromatic rings. Interestingly proton exchange is observed between H1, H7, and OH. These two latter protons are in the fast-exchange regime and result in a single signal in the explored temperature range, while H1 (that at low temperature moves at low field, likely involved in a hydrogen bond interaction with the OH group of the borate moiety) is in slow exchange with them at 223 K as shown in a 2D [¹H–¹H] EXSY/NOESY experiment (Figure S10). Similar behavior can be observed in dichloromethane at comparable temperatures. However, overcooling of the sample (below 173 K) results in the H7/OH exchange being slowed enough to observe, in the ¹H spectrum, the H7 resonance at +16.46 ppm, while the three ¹⁹F resonances appear to be broadened.

(12) Vagedes, D.; Erker, G.; Kehr, G.; Bergander, K.; Kataeva, O.; Frölich, R.; Grimme, S.; Mück-Lichtenfeld, C. *Dalton Trans.* **2003**, 1337.

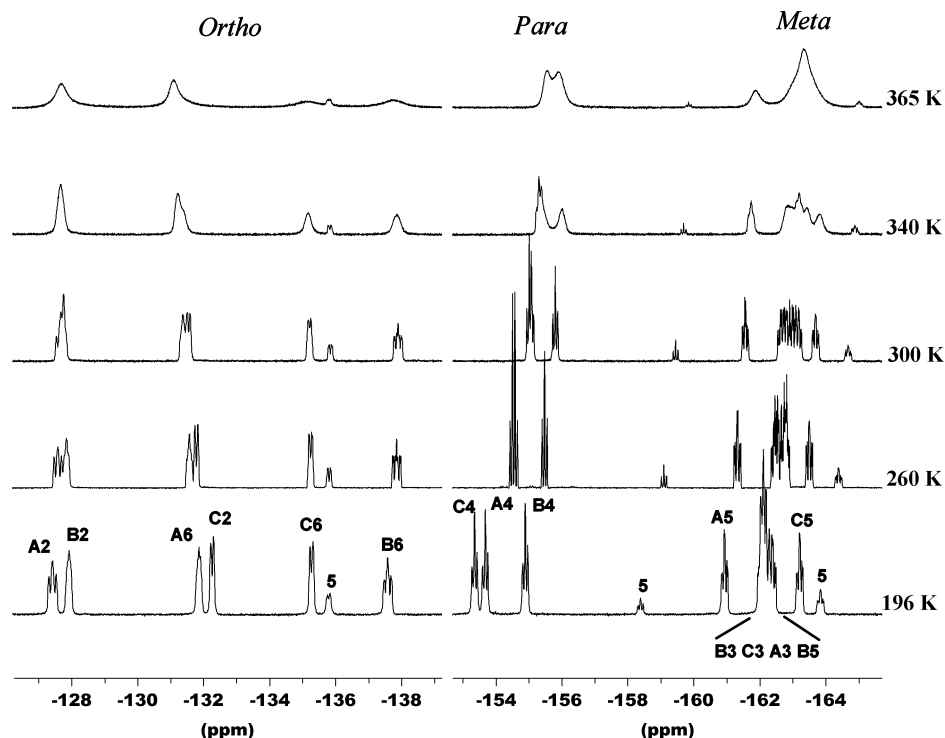


Figure 2. Variable temperature ^{19}F NMR spectra of **4** (7.1 T, toluene- d_8). The resonances are labeled according to Figure 3.

3. Solution Dynamics of Adduct 4. The ^{19}F variable-temperature spectra suggest the presence of dynamic processes, which eventually lead to the dynamic equivalence of the three perfluorinated rings. [^{19}F – ^{19}F] EXSY experiments have been performed at different temperatures and the analysis of the observed exchange cross-peaks pointed to two distinct processes.

At 275 K, the main process involves rings B and C (see the cross-peaks B2–C2, B2–C6, B6–C2, and B6–C6 in Figure 4a) leading to the exchange of the *in-plane* location of two rings. At this temperature, the enantiomerization process occurs through a ring A flip,¹³ rotation of rings B and C around their B–C_{ipso} bonds, together with a small rotation around the B–N interaction of the heterocyclic moiety. When the temperature is increased to 283 K, exchange cross-peaks between the ring A and C resonances became clearly observable as shown in the meta region by A5–C3 and A5–C5 exchange cross-peaks¹⁴ (Figure 4b), indicating the onset of wider rotations around the B–N bond. No exchange cross-peak is detectable between the signals of the A and B rings up to 305 K.

Therefore rotation around B–N bond is not free, likely hindered by the interactions between the two protons H6 and H1 with four of the *ortho*-fluorine atoms. It should be noted that in the B/C exchange three out of the four H···F interactions have to interchange.

The activation parameters for the B/C and A/C exchanges, reported in Table 3, have been calculated from the rate

(13) Brocas, J.; Gielen, M.; Willem R. In *The Permutational Approach to Dynamic Stereochemistry*; McGraw-Hill University Press: Cambridge, U.K., 1983.

(14) A3–C3 and A3–C5 cross-peaks are hidden by the stronger cross-peaks from the B/C exchange.

Table 3. Activation Parameters Obtained for the Two Dynamic Processes Observed in Some *N*-Heterocycle-B(C₆F₅)₃ Adducts

adduct	exchange process	E_a (kJ/mol)	$\ln A$	ΔH^\ddagger (kJ/mol)	ΔS^\ddagger (kJ/mol K)
4	B–C	69(3)	28(1)	66(3)	–18(10)
	A–C	78(5)	31(2)	76(5)	–5(18)
2	B–C	69.7(6)	31.6(2)	67.1(5)	9.3(2)
	A–B ^a	75.3(9)	31.3(3)	72.6(9)	7(3)
7	B–C	60(1)	29(0.7)	58(1)	–12(5)
	A–C	72(3)	31(1)	69(3)	2(20)

^a In compound **2**, the ring labeled C is the one that adopts the *in-plane* conformation.

constants estimated through the analysis of several 2D [^{19}F – ^{19}F] EXSY experiments¹⁵ and plotted in Figure 5.

The dynamic behavior of compound **4** is similar to that of the (C₆F₅)₃B-indole adduct (**2**),⁷ and the activation parameters of the two processes are comparable (see Table 3). Likely, in the two compounds, the rotation hindrance experienced by the perfluoroaryl and heterocyclic moieties is similar, being in both cases engaged in four H···F intramolecular interactions.

The relevance of these interactions is supported by the comparison with the dynamic behavior of other (C₆F₅)₃B-*N*-heterocycle adducts. For instance if we compare compound **2** with the (C₆F₅)₃B-anthranil complex (**6**, Scheme 7) where the nitrogen is the boron binding site, no interaction can be established between position 2, occupied by an oxygen atom,

(15) The close contacts between some of the *ortho*-fluorines causes the appearance of the *J* and *nOe* contributions to the cross-peaks observed in EXSY experiments. Therefore their values are not reliable for quantitative measurements, but in a series of experiments at the same temperature with different mixing times, they can be used qualitatively to detect exchange processes. For the quantitative volume analysis, we have taken into account the exchange cross-peaks of the meta region.

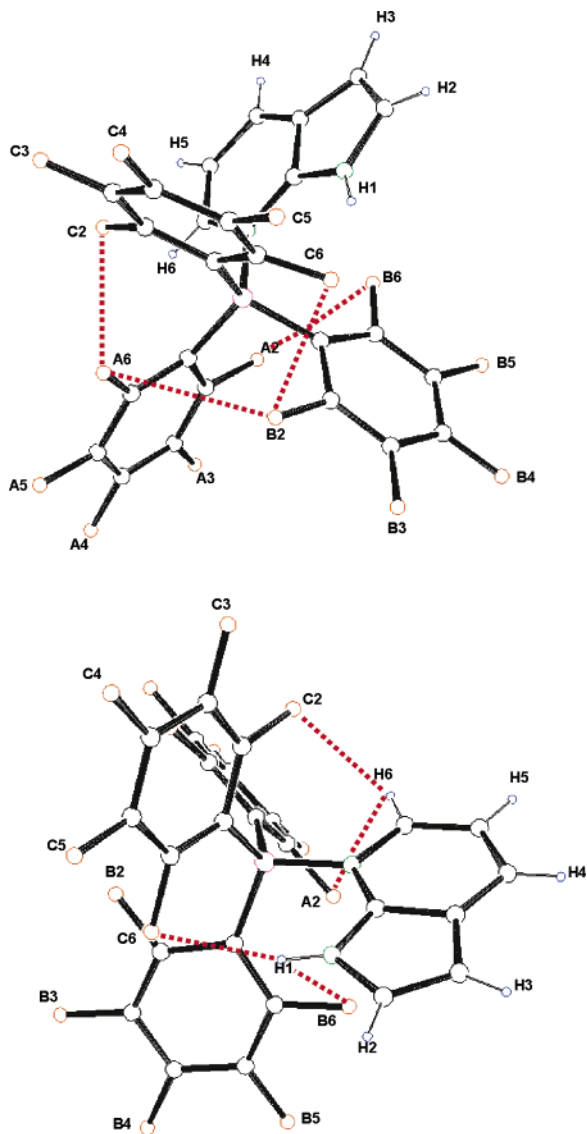


Figure 3. Two views of the solution structure of **4** as derived from 2D ^{19}F - ^{19}F and ^{19}F - 1H correlation experiments. The experimental dipolar and scalar interactions are indicated with dotted lines.

and the fluorine atoms of the $B(C_6F_5)_3$ moiety. Indeed the variable-temperature ^{19}F spectra of **6** show a single set of signals at room temperature, and even at 200 K, the exchange of two rings is fast on the NMR time scale (Figure S11). The dynamic behavior of pyrrole adducts fit nicely into this view, while for $(C_6F_5)_3B$ -pyrrole (**1**), free rotation around the B-C and B-N bonds is observed at temperatures as low as 173 K;⁷ for the *N*- $[(C_6F_5)_3B]$ -2,4-dimethylpyrrole adduct (**7**, Chart 1),⁷ the interactions between Me2 and the fluorine B6 (Figure 6) and between 5' and A2 (data not shown) make both the *in-plane* interchange and the B-N rotation slower. However the smaller activation parameters indicate that these interactions are less effective than in **4** and **2**.

Among these $H\cdots F$ interactions, only the one between N-H and fluorine C6 in complex **4** (see Figure 3) can be described as a hydrogen bond. For all the others, the observation of a scalar or dipolar coupling between the *ortho*-fluorines and carbon-bound hydrogens does not imply any

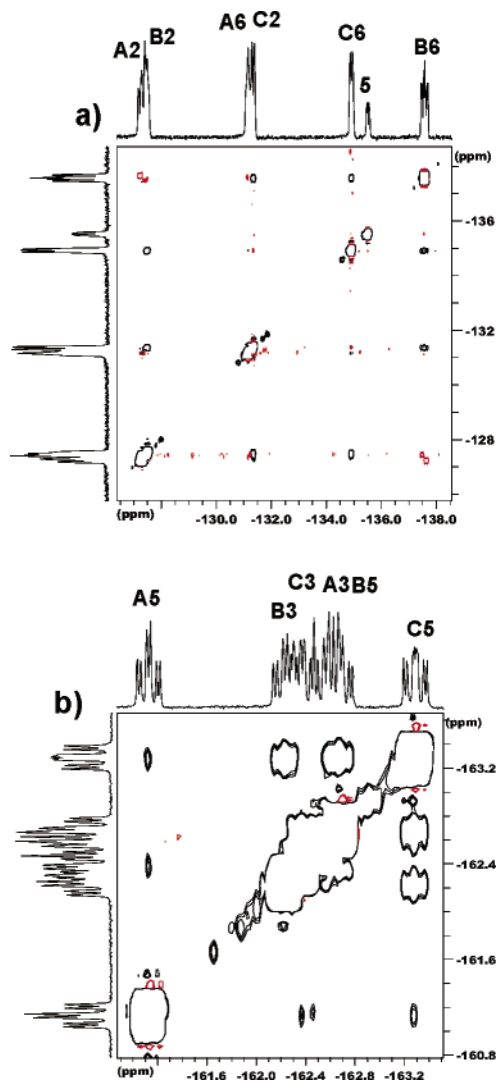


Figure 4. Selected regions of a 2D $[^{19}F$ - $^{19}F]$ EXSY/NOESY experiment of **4** (7.1 T, $\tau_m = 0.1$ s, red peaks = nOe, black peaks = exchange, toluene- d_6): (a) ortho region (275 K) and (b) meta region (283 K).

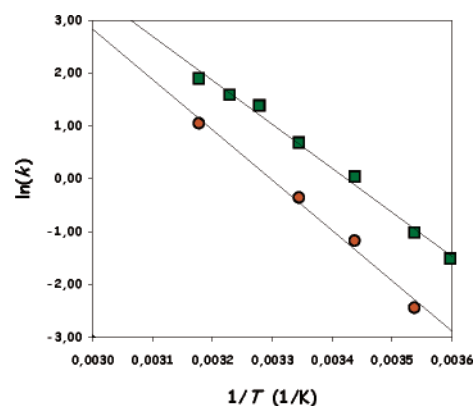


Figure 5. Arrhenius plot of the rate constants for the dynamic processes observed for compound **4**: exchange of B/C rings (\square) and exchange of A/C rings (\circ).

positive polarization of these hydrogen atoms, it simply shows the spatial proximity of these nuclei.¹⁶

Interestingly the activation data found in the present study are higher than those reported by Erker and co-workers¹² for the $(C_6F_5)_3B$ -*N*-methylbenzimidazole adduct. Smaller

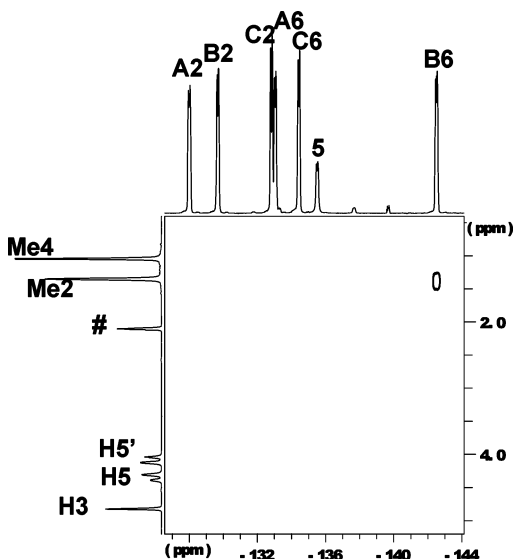


Figure 6. $[^1\text{H}-^{19}\text{F}]$ COSY of **7** (203 K, 7.1 T, $J_{\text{H-F}} = 4$ Hz, # indicates toluene).

Scheme 7

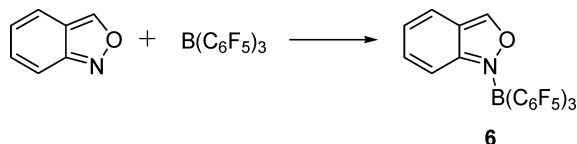
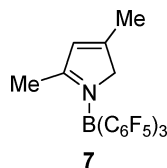


Chart 1



activation parameters have also been reported by Piers and co-workers¹⁸ for $(\text{C}_6\text{F}_5)_3\text{B-N}$ -benzylimine adducts where the barrier for the rotation was attributed to the π -stacking interaction between the positively polarized benzylic ring and one of the negatively polarized perfluorinated rings.

4. Solid State Structures of 4 and 5. The molecular structures of the complex of 7-aza-1*H*-indole with tris(pentafluorophenyl)borane (**4**) and of the 7-aza-1*H*-indolium hydroxotris(pentafluorophenyl)borate ion pair (**5**) have been determined in the solid state by X-ray diffraction analysis. Figures 7 and 8 show an ORTEP view of complexes **4** and **5**, respectively. Tables 4 (distances) and 5 (angles) contain the most relevant bonding parameters for the two compounds. Details of the inter- and intramolecular hydrogen bonds for compounds **4** and **5** are reported in Table 6.

The formulation of **4** as an equimolecular adduct between 7-aza-1*H*-indole and tris(pentafluorophenyl)borane is con-

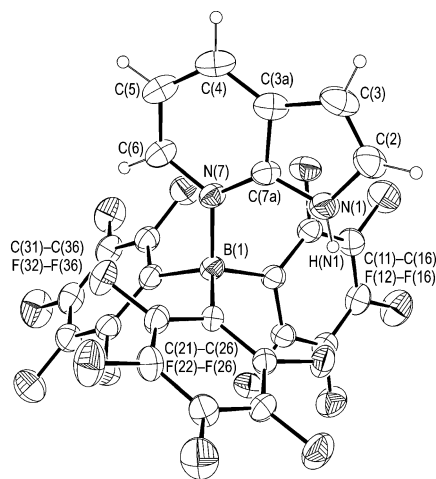


Figure 7. ORTEP view of the structure of (7-aza-1*H*-indole)tris(pentafluorophenyl)boron (**4**) with a partial labeling scheme. Thermal ellipsoids are drawn at the 30% probability level; hydrogen atoms are given arbitrary radii. Only one of the two independent molecules is shown.

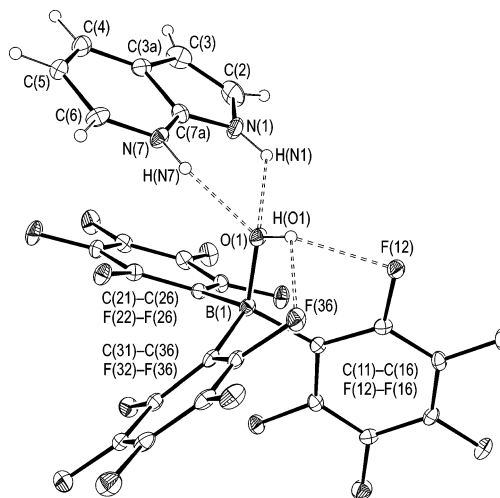


Figure 8. ORTEP view of the structure of the 7-aza-1*H*-indolium hydroxotris(pentafluorophenyl)borate ion pair (**5**) with a partial labeling scheme. Thermal ellipsoids are drawn at the 30% probability level; hydrogen atoms are given arbitrary radii. Only the major disordered component of the azaindolum cation is shown.

firmed. The neutral azaindole ligand usually coordinates through the pyridine nitrogen atom N(7), whereas the anionic azaindolato ligand binds through the indole nitrogen atom N(1) or bridges by means of a $\mu\text{-}\kappa\text{N}^1:\kappa\text{N}^7$ coordination mode.¹⁹ In accordance with these observations, in **4** the azaindole assumes a κN^7 coordination mode.

In this class of compounds, boron–nitrogen bond distances show a sensible dependence on the electronic and steric environment, in particular short bond distances usually correlate with the presence of unhindered strong bases. The B(1)–N(7) distance in **4** (1.608 Å, mean value) is similar to the B–N distances found in other pyridine derivatives such as **3** (1.628 Å),⁶ the 4-(NMe_2)pyridine adduct (1.604 Å), and

(16) Bona fide intramolecular hydrogen bonds have been observed in adducts between $\text{B}(\text{C}_6\text{F}_5)_3$ and primary and secondary amines.¹⁷ The $\text{N-H}\cdots\text{F}-\text{C}$ hydrogen bonds make rotation around the B atom hindered enough to allow the observation of separate resonances for the three perfluorinated rings at room temperature or slightly below.

(17) (a) Lancaster, S. J.; Mountford, A. J.; Hughes, D. L.; Schormann, M.; Bochmann, M. *J. Organomet. Chem.* **2004**, *680*, 193. (b) Mountford, A. J.; Lancaster, S. J.; Coles, S. J.; Horton, P. N.; Hughes, D. L.; Hursthouse, M. B.; Light, M. E. *Inorg. Chem.* **2005**, *44*, 5921.

(18) Blackwell, J. M.; Piers, W. E.; Parvez, M.; McDonald, R. *Organometallics* **2002**, *21*, 1400.

(19) (a) Dufour, P.; Dartiguenave, Y.; Dartiguenave, M.; Dufour, N.; Lebus, A.-M.; Bélanger-Gariépy, F.; Beauchamp, A.-L. *Can. J. Chem.* **1990**, *68*, 193. (b) Dufour, N.; Lebus, A.-M.; Corbeil, M.-C.; Beauchamp, A.-L.; Dufour, P.; Dartiguenave, Y.; Dartiguenave, M. *Can. J. Chem.* **1992**, *70*, 2914. (c) Wu, Q.; Esteghamatian, M.; Hu, N.-X.; Popovic, Z.; Enright, G.; Breeze, S. R.; Wang, S. *Angew. Chem., Int. Ed.* **1999**, *38*, 985.

Table 4. Selected Bond Distances (Å) for **4** and **5**^a

	4		5
	I	II	
N(1)–C(2)	1.385(3)	1.382(3)	1.395(6)
N(1)–C(7a)	1.343(3)	1.354(3)	1.339(7)
C(2)–C(3)	1.321(4)	1.339(3)	1.366(7)
C(3)–C(3a)	1.424(4)	1.416(3)	1.442(7)
C(3a)–C(4)	1.386(3)	1.367(3)	1.376(6)
C(3a)–C(7a)	1.407(3)	1.401(3)	1.433(5)
C(4)–C(5)	1.373(3)	1.379(3)	1.386(7)
C(5)–C(6)	1.381(3)	1.375(3)	1.378(7)
C(6)–N(7)	1.350(3)	1.354(3)	1.353(6)
N(7)–C(7a)	1.353(3)	1.357(3)	1.345(7)
X ^b –B(1)	1.605(3)	1.612(3)	1.500(3)
B(1)–C(11)	1.658(3)	1.649(3)	1.660(3)
B(1)–C(21)	1.640(3)	1.643(3)	1.662(3)
B(1)–C(31)	1.661(3)	1.637(3)	1.675(3)

^a I and II refer to the two independent molecules in the asymmetric unit of **4**·1/2CH₂Cl₂. Only the major disordered component of the 7-azaindolum cation in **5** is considered. ^b X = N(7) for **4**, and X = O(1) for **5**.

Table 5. Selected Bond and Torsion Angles (deg) for **4** and **5**^a

	4		5
	I	II	
C(2)–N(1)–C(7a)	108.5(2)	108.0(2)	107.9(3)
N(1)–C(2)–C(3)	109.8(2)	109.9(2)	109.9(4)
C(2)–C(3)–C(3a)	107.8(2)	107.5(2)	107.5(4)
C(3)–C(3a)–C(4)	136.5(3)	136.2(2)	138.0(4)
C(3)–C(3a)–C(7a)	105.8(2)	106.3(2)	104.4(5)
C(4)–C(3a)–C(7a)	117.7(2)	117.5(2)	117.6(5)
C(3a)–C(4)–C(5)	118.2(2)	118.9(2)	119.6(4)
C(4)–C(5)–C(6)	120.9(2)	120.6(2)	121.0(4)
C(5)–C(6)–N(7)	122.8(2)	122.7(2)	120.2(4)
C(6)–N(7)–C(7a)	115.92(19)	115.51(19)	120.2(4)
N(1)–C(7a)–C(3a)	108.1(2)	108.4(2)	110.3(4)
N(1)–C(7a)–N(7)	127.5(2)	126.8(2)	128.3(4)
C(3a)–C(7a)–N(7)	124.4(2)	124.8(2)	121.5(5)
C(6)–N(7)–B(1)	123.45(19)	123.10(19)	
C(7a)–N(7)–B(1)	120.56(18)	120.96(19)	
X ^b –B(1)–C(11)	110.62(18)	111.16(18)	113.45(17)
X–B(1)–C(21)	103.16(18)	101.44(17)	100.96(16)
X–B(1)–C(31)	110.88(17)	112.36(18)	110.19(16)
C(11)–B(1)–C(21)	114.92(18)	116.04(19)	113.67(17)
C(11)–B(1)–C(31)	102.22(18)	102.80(18)	105.15(16)
C(21)–B(1)–C(31)	115.25(19)	113.42(19)	113.65(17)
X ^b –B(1)–C(11)–C(12)	–16.4(3)	–19.1(3)	14.7(3)
X–B(1)–C(11)–C(16)	173.73(19)	171.33(19)	–169.06(17)
X–B(1)–C(21)–C(22)	–111.6(2)	–108.9(3)	95.9(3)
X–B(1)–C(21)–C(26)	64.1(2)	64.9(2)	–71.3(2)
X–B(1)–C(31)–C(32)	–130.1(2)	–133.7(2)	132.6(2)
X–B(1)–C(31)–C(36)	62.6(3)	56.2(3)	–45.6(3)

^a I and II refer to the two independent molecules in the asymmetric unit of **4**·1/2CH₂Cl₂. Only the major disordered component of the 7-azaindolum cation in **5** is considered. ^b X = N(7) for **4**, and X = O(1) for **5**.

the 4-[4'-(NMe₂)C₆H₄C≡C]pyridine adduct (1.620 Å).²⁰ This result could be related to a balance between the slightly lower basicity of 7-azaindole with respect to pyridine⁹ and the building up of some attractive NH···F hydrogen-bond interactions between the acidic indole NH proton and the *ortho*-fluorine substituents of the borane moiety.

Bond distances within the heterocyclic moiety in **4** compare well to those observed in the free azaindole molecule²¹ and are consistent with an extensive delocalization of the π -electrons in both the rings.

(20) Lesley, M. J. G.; Woodward, A.; Taylor, N. J.; Marder, T. B.; Cazenobe, I.; Ledoux, I.; Zyss, J.; Thornton, A.; Bruce, D.; Kakkar, K. *Chem. Mater.* **1998**, *10*, 1355.

Table 6. Intra- and Intermolecular Hydrogen-Bond Parameters (Å, deg) for **4** and **5**^a

	D–H	H···A	D···A	D–H···A
4				
N(1)–H(N1)···F(22)	0.860	2.310	3.135(3)	160.0
	0.860	2.320	3.095(3)	150.0
5				
O(1)–H(O1)···F(12)	0.840	2.193	2.769(2)	125.7
O(1)–H(O1)···F(36)	0.840	2.279	2.803(2)	120.7
N(1)–H(N1)···O(1)	0.860	2.390	2.977(5)	124.3
N(1)–H(N1)···F(13i)	0.860	2.367	3.098(5)	140.6
N(7)–H(N7)···O(1)	0.860	1.977	2.732(4)	143.0
N(7)–H(N7)···F(34ii)	0.860	2.657	3.254(4)	126.1

^a For each interaction in **4**, we report two values related to the two independent molecules in the asymmetric unit of **4**·1/2CH₂Cl₂. Only the major disordered component of the 7-azaindolum cation in **5** is considered. Symmetry operations: (i) 1 – x, 1 – y, 2 – z; (ii) 1 – x, 1 – y, 1 – z.

As far as **5** is concerned, the structure of the [B(C₆F₅)₃OH][–] anion is similar to the previously determined ones,²² in particular the hydrogen atom of the hydroxo group is involved in a bifurcated hydrogen bond with two *ortho*-fluorine atoms of two different pentafluorophenyl rings, whereas the oxygen atom acts as a hydrogen-bond acceptor for both the N–H groups of the cation (see Figure 8 and Table 6). The azaindolum cation is disordered, as in most of its previously determined structures.²³ Disorder is often observed in the crystals of compounds containing fused five- and six-member rings, for which the two halves of the molecule show a near equivalence of the van der Waals and electrostatic potential envelopes.

As can be seen from Figures 7 and 8 and from the torsion angles reported in Table 5, in both complexes **4** and **5** the B(C₆F₅)₃ moiety adopts a very similar conformation. In particular, one of the three phenyl rings, the so-called *in-plane* ring, labeled C(11–16), almost eclipses the B–N or the B–O bond, whereas the other two exhibit a two-bladed propeller-like conformation. This very same conformation can be found in most of the crystal structures of tris(pentafluorophenyl)borane derivatives collected in the Cambridge Structural Database;²⁴ from this evidence, it can be inferred that this molecular fragment is very rigid, so that the presence of a high energy barrier to the enantiomerization process of the chiral moiety can be expected. It must be noted that this arrangement of the pentafluorophenyl rings does not seem to be a consequence of the formation of any particular non-bonded or hydrogen-bonded interaction between the B(C₆F₅)₃ moiety and the rest of the molecule because it can be observed even in adducts with sterically undemanding ligands, not bearing any acidic hydrogen atoms.

- (21) Mean bond distances (Å) for the 7-azaindole molecule are as follows: N(1)–C(2) = 1.370(5), N(1)–C(7a) = 1.361(4), C(2)–C(3) = 1.342(5), C(3)–C(3a) = 1.419(5), C(3a)–C(4) = 1.383(6), C(3a)–C(7a) = 1.398(5), C(4)–C(5) = 1.377(6), C(5)–C(6) = 1.375(5), C(6)–N(7) = 1.337(5), N(7)–C(7a) = 1.341(4).^{19a}
- (22) (a) Bergquist, C.; Parkin, G. *J. Am. Chem. Soc.* **1999**, *121*, 6322. (b) Duchateau, R.; van Santen, R. A.; Yap, G. P. A. *Organometallics* **2000**, *19*, 809. (c) Stibrany, R. T.; Brant, P. *Acta Crystallogr., Sect. C* **2001**, *57*, 644. (d) Bergquist, C.; Fillebeen, T.; Morlok, M. M.; Parkin, G. *J. Am. Chem. Soc.* **2003**, *125*, 6189.
- (23) (a) Sheldrick, W. S. *Z. Naturforsch., B* **1982**, *37*, 653. (b) Poitras, J.; Leduc, M.; Beauchamp, A.-L. *Can. J. Chem.* **1993**, *71*, 549.
- (24) CSD, version 5.26; November 2004. Allen, F. H. *Acta Crystallogr., Sect. B* **2002**, *58*, 380.

Table 7. Selected F...F and F...H Distances (Å) for **4**^a

	F(22)	F(26)	F(32)	F(36)	H(N1)	H(6)
F(12)	4.550(3)	5.618(3)	6.056(3)	2.828(2)	3.11	4.07
	4.617(3)	5.602(3)	5.987(3)	2.852(2)	3.08	4.08
F(16)	2.733(2)	4.812(3)	3.209(2)	4.519(3)	4.08	5.36
	2.738(2)	4.773(3)	2.940(2)	4.651(3)	4.03	5.40
F(22)			4.557(3)	5.631(4)	2.18	5.75
			4.373(3)	5.718(3)	2.19	5.74
F(26)			2.749(2)	4.868(3)	4.61	2.91
			2.879(2)	4.657(3)	4.74	2.79
F(32)					5.40	4.14
					5.35	4.32
F(36)					4.91	2.70
					4.90	2.57

^a Close contacts are indicated in bold (the sum of the van der Waals radii for the F...F and F...H contacts are 3.0 and 2.7 Å, respectively). For each interaction, we report two values related to the two independent molecules in the asymmetric unit of **4**·1/2CH₂Cl₂. N–H and C–H bond distances are normalized to 1.009 and 1.083 Å, respectively.³¹

This conformation eventually implies some short F...F non-bonded contacts between the *ortho*-fluoro substituents of the three phenyl rings, and in the case of adduct **4**, some F...H contacts involving the hydrogen atoms bound to N(1) and C(6). A list of these interactions for compound **4**, (in which they are revealed also in solution, at low temperature, by NMR spectroscopy) is reported in Table 7.

Conclusions

Pyridine removes the borane from the complexes (C₆F₅)₃B-pyrrole (**1**) and (C₆F₅)₃B-indole (**2**) releasing pyrrole or indole and giving the more stable adduct (C₆F₅)₃B-pyridine (**3**). The preference of B(C₆F₅)₃ for the pyridinic moiety is exemplified in the reaction between the borane and 7-azaindole which leads to a stable adduct (**4**), where the borane is coordinated to the pyridinic nitrogen. The competition between pyridine and 7-azaindole for the coordination with B(C₆F₅)₃ has been studied as well.

The B(C₆F₅)₃ moiety in the solid-state structures of compounds **4** and **5** shows a typical conformation, found by now in more than 40 adducts, taking into account nitrogen-containing derivatives only.⁶

In neutral adducts, this conformation also drives the arrangement of the heterocyclic moiety with respect to the borane fragment. This can result in intramolecular contacts that, as in the case of **4**, contribute to the activation barriers for the rotation of the substituents around boron atom and make it slow enough to allow the determination through NMR spectroscopy both of the solution structure and of the nature and energetics of these dynamic processes.

Experimental Section

General Procedures and Starting Materials. All operations were performed under nitrogen using conventional Schlenk-line techniques. Solvents were purified by degassing with N₂ and passing over activated (8 h, N₂ purge, 300 °C) Al₂O₃, and they were stored under nitrogen. Indole (Aldrich or Fluka), pyridine, 7-azaindole, 2,5-dimethylpyrrole, anthranil (Aldrich), and B(C₆F₅)₃ (Boulder Scientific Company) were used as received. Compound H₂O–B(C₆F₅)₃ was synthesized as reported in a previous publication.⁷

EI-MS spectra were recorded on a VG 7070 EQ spectrometer operating at 70 eV.

The samples for NMR studies were dissolved in CD₂Cl₂ (Aldrich, 99.8% atom D), CDCl₃ (Aldrich, 99% atom D), or C₇D₈ (CIL, 99.5% atom D); all were dried over activated 4 Å molecular sieves before use. The ¹H and ¹³C NMR spectra obtained using a Bruker DPX 200 spectrometer were acquired with a 15° pulse and 2 s of delay for ¹H and with a 45° pulse and 6 s of delay for ¹³C.

NMR dynamic studies in toluene solutions were performed on a Bruker DRX 300 spectrometer equipped with a QNP probehead (90° ¹H = 10 μs, 90° ¹⁹F = 10 μs, 90° ¹³C = 7 μs); ¹¹B and ¹⁵N NMR spectra were recorded on a Bruker DRX 400 equipped with a BBI probehead (90° ¹¹B = 22 μs, ¹⁵N = 29 μs). ¹⁹F NMR spectra were referenced to external CFC₃ (δ = 0 ppm), and the ¹¹B NMR spectra were referenced to external Et₂O·BF₃ (δ = 0 ppm), while ¹⁵N NMR spectra were referenced to external CH₃NO₂ (δ = 0 ppm).

All the NMR data reported here were acquired at 298 K, if not otherwise specified. The temperature was calibrated with a standard CH₃OH/CD₃OD solution for the range of 188–300 K.²⁵

N-[Tris(pentafluorophenyl)borane]-pyridine (3**).** A solution of pyridine (0.37 g, 4.68 mmol) in 3 mL of dichloromethane was added at room temperature to a solution of B(C₆F₅)₃ (2.39 g, 4.67 mmol) in 15 mL of dichloromethane. A light exothermicity was observed. After the mixture was stirred for 30 min at room temperature, the solvent was evaporated under reduced pressure to give a white solid (quantitative yield). ¹H NMR (CD₂Cl₂): δ 7.06–7.13 (m, 2H, *H3* and *H5*), 7.42–7.52 (m, 1H, *H4*), 8.51–8.55 (m, 2H, *H2* and *H6*). ¹³C NMR (CD₂Cl₂): δ 123.45 (*C3* and *C5*), 135.54 (*C4*), 149.80 (*C2* and *C6*).

7-[Tris(pentafluorophenyl)borane]-7-azaindole (4**).** A solution of 7-azaindole (0.57 g, 4.7 mmol) in 10 mL of dichloromethane was added at room temperature to a solution of B(C₆F₅)₃ (2.43 g, 4.7 mmol) in 20 mL of dichloromethane. A light yellow solution was obtained; after the mixture was stirred for 1 h, the solvent was removed in a vacuum to give a white solid (quantitative yield). Anal. Calcd for C₂₅H₆BF₁₅N₂: C, 47.7; H, 0.960; N, 4.45. Found: C, 47.64; H, 1.12; N, 3.83. EI-MS: *m/z* 630.0 (C₆F₅)₃B-7-N₂C₇H₆. ¹H NMR (CDCl₃): δ 6.73 (dd, 1H, *J* = 3.67 Hz, *J* = 1.96 Hz, *H3*), 7.32 (dd, 1H, *J* = 3.67 Hz, *J* = 2.45 Hz, *H2*), 7.38 (dd, 1H, *J* = 7.34 Hz, *J* = 6.85 Hz, *H5*), 8.36 (m, 2H, *H4* and *H6*), 9.02 (bs, 1H, *NH*). ¹³C NMR (CD₂Cl₂): δ 103.59 (*C3*), 115.76 (*C5*), 125.10 (*C3a*), 126.56 (*C2*), 135.91 (*C4*), 139.12 (*C6*), 142.76 (*C7a*).

For the structural and dynamic studies, generally a colorless solution of **4** was prepared by dissolving ca. 20–25 mg in an NMR tube containing C₇D₈. ¹H NMR (300 K, C₇D₈): δ 8.74 (br s, 1H, *J* = 2.02 Hz, *J* = 2.6 Hz, *H1*), 8.08 (m, 1H, *J* = 6.13 Hz, *H6*), 7.28 (d, 1H, *J* = 7.67 Hz, *H4*), 6.48 (dd, 1H, *J* = 6.13 Hz, *J* = 7.67 Hz, *H5*), 6.11 (dd, 1H, *J* = 3.75 Hz, *J* = 2.02 Hz, *H2*), 5.93 (dd, 1H, *J* = 3.75 Hz, *J* = 2.6 Hz, *H3*). ¹³C NMR (C₇D₈) (Figure S12): δ 142.71 (*C7'*), 138.90 (*C6*), 135.61 (*C4*), 126.00 (*C2*), 125.00 (*C3'*), 115.43 (*C5*), 103.42 (*C3*). ¹⁹F NMR chemical shifts are reported in Table 1. ¹¹B NMR (C₇D₈): δ –5.17 (br s). ¹⁵N NMR (213 K, C₇D₈): δ –186 (*N7*), –251 (*N1*).

The rate constants for the exchanges of rings B/C and A/C estimated by volume analysis of 2D ¹⁹F EXSY experiments are the following: B/C *k* (T) 0.22 (278), 0.36 (283), 1.04 (291), 1.98 (299), 4.00 (305), 4.89 (310), 6.67 s^{–1} (315 K); A/C *k* (T) 0.087 (283), 0.31 (291), 0.70 (299), 2.86 s^{–1} (315 K).

Reaction of **4 with Pyridine.** A CD₂Cl₂ solution of compound **4** (60.6 mg in 1.21 mL, 0.0795 M) was prepared and transferred under a nitrogen atmosphere into two NMR tubes. Different

amounts of pyridine (1 and 5 equiv) were added at low temperature (193 K) to the two samples. ¹⁹F NMR spectra were acquired at 298 K at different times on both the samples to monitor the exchange reaction. The resulting data are shown in Figure S1.

Reaction of 7-Azaindole with H₂O–B(C₆F₅)₃. In a 5 mm NMR tube, H₂O–B(C₆F₅)₃ (23 mg, 43 μmol) was added at room temperature to a solution of 7-azaindole (5.2 mg, 43 μmol) in 1 mL of CD₂Cl₂ to give a light yellow solution. The reaction was monitored via ¹H NMR at different times. Complex **5** was instantaneously and quantitatively formed, as shown by spectroscopic monitoring, and slowly converted into complex **4**. According to the spectra area values, the following percentages on compound **4** with respect to **5** were registered: 20:80 after 30 min, 36:64 after 1.5 h, 51:49 after 3.1 h, 54:46 after 4.7 h, and 67:33 after almost 24 h. The latter value did not change with time, remaining unchanged even after two weeks. An excess of H₂O was added to the mixture, but the ratio **4/5** was not altered and remained approximately 2:1. [7-azaindolum]⁺[HOB(C₆F₅)₃][−] (**5**). ¹H NMR (CD₂Cl₂): δ 6.84 (d, 1H, *J* = 3.52 Hz, *H3*), 7.43–7.50 (m, 1H, *H5*), 7.56 (d, 1H, *J* = 3.52 Hz, *H2*), 7.84 (bs, 2H, *OH* and *NH7*), 8.08 (d, 1H, *J* = 5.87 Hz, *H6* or *H4*), 8.52 (d, 1H, *J* = 7.83 Hz, *H4* or *H6*), 10.01 (bs, 1H, *NH1*). ¹H NMR (220 K, CD₂Cl₂): δ 6.72 (d, 1H, *J* = 3.5 Hz, *H3*), 7.36 (dd, *J* = 7.8, 5.6 Hz, 1H, *H5*), 7.40 (1H, *H2*), 7.84 (bs, 2H, *OH* and *NH7*), 8.06 (d, 1H, *J* = 5.87 Hz, *H6*), 8.36 (1H, *H4*), 11.73 (bs, 1H, *NH1*). The resonances of *H2* and *H4*, assigned through a 2D NOESY/EXSY experiment, lie under signals of **4**, also present in solution. ¹H NMR (168 K, CD₂Cl₂): δ 6.63, 7.20, 7.94, 12.73, 16.46; the other resonances are overlapped by the signals of compound **4**. ¹⁹F NMR (168 K, CD₂Cl₂): δ −135.94 (6F *ortho*, Δ*v*_{1/2} = 208 Hz), −159.32 (3F *para*, Δ*v*_{1/2} = 90 Hz), −164.34 (6F *meta*, Δ*v*_{1/2} = 72 Hz). ¹H NMR (233 K, C₇D₈): δ 6.09 (d, 1H, *J* = 3.20 Hz, *H3*), 6.25 (bs, 2H, *OH* and *NH7*), 6.44 (dd, 1H, *J* = 5.03 Hz, *J* = 7.77 Hz, *H5*), 6.60 (d, 1H, *J* = 3.20 Hz, *H2*), 7.32 (d, 1H, *J* = 7.77 Hz, *H4*), 7.59 (d, 1H, *J* = 5.03 Hz, *H6*), 11.11 (bs, 1H, *NH1*). ¹⁹F NMR (233 K, C₇D₈): δ −135.47 (*ps* dd, 6F *ortho*), −158.62 (t, 3F *para*), −163.89 (m, 6F *meta*). ¹¹B NMR (C₇D₈): δ −3.60 (br s).

N-[Tris(pentafluorophenyl)borane]-anthranil (6**).** A solution of anthranil (99%, 0.446 g, 3.71 mmol) in 5 mL of toluene was added at room temperature under a nitrogen atmosphere to a solution of tris(pentafluorophenyl)borane (99.4%, 1.914 g, 3.72 mmol) in 15 mL of toluene. Exothermicity was not observed. During the addition, the color of the solution turned from light yellow to dark yellow. The reaction mixture was stirred for 1 h at room temperature, and then the solvent was evaporated in vacuo to give a yellow powder (yield 98%). Anal. Calcd for C₂₅H₅BF₁₅NO: C, 47.6; H, 0.800; N, 2.22. Found: C, 47.8; H, 0.94; N, 1.98. EI-MS: *m/z* 631.0 (C₆F₅)₃B – NOC₇H₅. ¹H NMR (C₆D₆): δ 6.30 (ddd, 1H, *J* = 9.00 Hz, *J* = 6.65 Hz, *J* = 0.78 Hz, *H5* or *H6*), 6.52 (dt, 1H, *J* = 9.00 Hz, *J* = 1.17 Hz, *H4*), 6.62 (ddd, 1H, *J* = 9.00 Hz, *J* = 6.65 Hz, *J* = 1.17 Hz, *H6* or *H5*), 6.94 (bd, 1H, *J* = 9.00 Hz, *H7*), 7.17 (d, 1H, *J* = 0.98 Hz, *H3*). ¹³C NMR (C₆D₆): δ 111.54 (*C7*), 119.67 (*C7a* or *C3a*), 120.89 (*C4*), 126.59 (*C5* or *C6*), 137.64 (*C6* or *C5*), 149.77 (*C3a* or *C7a*), 156.66 (*C3*).

The variable-temperature spectra were recorded on a solution prepared by dissolving 39 mg (0.063 mmol) of **6** in 0.6 mL of C₇D₈ (0.104 M) at room temperature. The solution appeared to be beige and transparent. ¹H NMR (300 K, C₇D₈): δ 7.05 (overlapped to a toluene signal 1H, *H7*), 6.97 (d, 1H, *H3*), 6.48 (dd, 1H, *H5/6*), 6.42 (d, 1H, *H4*), 6.21 (dd, 1H, *H5/6*). ¹⁹F NMR (188 K, C₇D₈): δ *ortho* −129.74 (br s, 1F), −130.48 (*ps* d, 1F), −133.11 (*ps* d, 1F), −134.68 (br s, 1F), −138.52 (br s, 1F); *para* −154.44 (br s,

1F), −155.01 (t, 1F), −155.60 (br s, 1F); *meta* −162.29 (m, 1F), −162.69 (br, 3F), −163.41 (br s, 1F), −163.78 (br s, 1F).

N-[Tris(pentafluorophenyl)borane]-2,4-dimethyl-5H-pyrrole (7**).** Thirty milligrams of adduct **7** (0.0494 mmol), prepared according to literature procedures,⁷ was dissolved in 0.7 mL of C₈D₇ in the NMR tube. The solution appears to be yellow and clear. ¹H NMR (C₈D₇): δ 1.28 (s, 3H, *CH*₃ in 4), 1.52 (br t, 3H, *CH*₃ in 2), 4.30 (broad AB system, 2H, *H5,H5'*), 5.15 (s, 1H, *J* = 1.57 Hz, *H3*). ¹⁹F NMR (300 K, C₈D₇): δ ring A 127.78 (m, *ortho*), −132.16 (m, *ortho*), −155.57 (*ps-t*, *para*), −161.83 (m, *meta*), −163.37 (m, *meta*); ring B −128.90 (br s, *ortho*), −142.10 (br s, *ortho*), −157.32 (br s, *para*), −163.68 (br s, *meta*), −164.57 (br s, *meta*); ring C −132.49 (br s, *ortho*), −133.88 (br s, *ortho*), −156.59 (br s, *para*), −163.23 (br s, *meta*), −164.24 (br s, *meta*). ¹¹B NMR (C₇D₈): δ −8.25 (br s).

The rate constants for the exchanges of rings B/C and A/C estimated by volume analysis of 2D ¹⁹F EXSY experiments are as follow: B/C *k* (T) 0.160 (235), 0.760 (247), 1.14 (251), 2.58 (259), 5.79 (265), 9.25 s^{−1} (271 K); A/C *k* (T) 0.125 (265), 0.302 (271), 0.580 (277), 1.25 (284), 1.82 s^{−1} (289 K).

X-ray Crystal Structure Analysis. Suitable crystals of **4**·1/2CH₂Cl₂ were obtained by cooling a solution of **4** in anhydrous dichloromethane for several months at −25 °C. Crystals of **5**, instead, grew at −5 °C in few days in either toluene solutions of **4** and **5** or solutions of **4** in nonanhydrous toluene. The crystals were mounted in air on a glass fiber tip onto a goniometer head. Single-crystal X-ray diffraction data were collected on a Siemens SMART CCD area detector diffractometer using graphite-monochromated Mo Kα radiation (λ = 0.71073 Å). Data collection was performed at room temperature for **4**·1/2CH₂Cl₂ and at 100 K for **5**, to obtain a better data set for the latter disordered phase.

Unit cell parameters were initially obtained from about 100 reflections taken from 45 frames collected in three different ω regions and eventually refined against about 3000 reflections with 2° ≤ θ ≤ 25°.

A full sphere of reciprocal space was scanned by 0.3° ω step, collecting 1800 frames (the exposure times were 10 and 40 s for **4**·1/2CH₂Cl₂ and **5**, respectively). Intensity decay was monitored by re-collecting the initial 50 frames at the end of data collection and analyzing the duplicate reflections. After integration, an empirical absorption correction was made on the basis of the symmetry-equivalent reflection intensities measured (for **4**·1/2CH₂Cl₂, 25909 reflections with an average redundancy of 9.0; for **5**, 6674 reflections with an average redundancy of 3.1).²⁶

Crystal data and data collection parameters are summarized in Table 8.

The structures were solved by direct methods (SIR97²⁷) and subsequent Fourier synthesis; they were refined by full-matrix least-squares on *F*² (SHELX97²⁸) using all reflections. Scattering factors for neutral atoms and anomalous dispersion corrections were taken from the internal library of SHELX97. Weights were assigned to individual observations according to the formula *w* = 1/[σ²(*F*_o²) + (*aP*)² + *bP*], where *P* = (*F*_o² + 2*F*_c²)/3; *a* and *b* were chosen to give a flat analysis of variance in terms of *F*_o². Anisotropic parameters were assigned to all non-hydrogen atoms except for the minor disordered component of the 7-azaindolum cation in **5** (see below).

(26) Sheldrick, G. M. *SADABS*; Universität Göttingen: Göttingen, Germany, 1996.

(27) Altomare, A.; Burla, M. C.; Camalli, M.; Cascarano, G. L.; Giacovazzo, C.; Guagliardi, A.; Moliterni, A. G. G.; Polidori, G.; Spagna, R. *J. Appl. Crystallogr.* **1999**, *32*, 115.

(28) Sheldrick, G. M. *SHELX97*; Universität Göttingen: Göttingen, Germany, 1997.

Table 8. Summary of Crystal Data, Data Collection, and Structure Refinement Parameters for **4**·1/2CH₂Cl₂ and **5**

	4 ·1/2CH ₂ Cl ₂	5
formula	C ₂₅ H ₆ BF ₁₅ N ₂ ·1/2CH ₂ Cl ₂	C ₇ H ₁₇ N ₂ ⁺ ·C ₁₈ HBF ₁₅ O ⁻
fw	672.59	648.14
cryst syst	monoclinic	triclinic
space group	<i>P</i> 2 ₁ / <i>c</i> (No. 14)	<i>P</i> 1̄ (No. 2)
<i>a</i> (Å)	19.249(8)	8.094(4)
<i>b</i> (Å)	14.026(5)	9.890(4)
<i>c</i> (Å)	18.467(8)	15.091(5)
α (deg)		92.86(1)
β (deg)	94.32(1)	101.00(1)
γ (deg)		96.99(1)
<i>V</i> (Å ³)	4972(3)	1173.7(8)
<i>Z</i>	8	2
<i>F</i> (000)	2648	640
density (g cm ⁻³)	1.797	1.834
abs coeff (mm ⁻¹)	0.289	0.195
cryst color	colorless	colorless
θ range (deg°)	1.1–25.0	2.1–25.0
index ranges	–22 ≤ <i>h</i> ≤ 22 –16 ≤ <i>k</i> ≤ 16 –21 ≤ <i>l</i> ≤ 21	–9 ≤ <i>h</i> ≤ 9 –11 ≤ <i>k</i> ≤ 11 –17 ≤ <i>l</i> ≤ 17
intensity decay (%)	0	0
min. transmission factors	0.857	0.813
no. of measured reflns	66355	12353
no. of independent reflns	8770	4136
<i>R</i> _{int} , <i>R</i> _σ ^a	0.0525, 0.0309	0.0352, 0.0363
no. of reflns with <i>I</i> > 2σ(<i>I</i>)	5334	3093
no. of data/restraints/params	8770/0/775	4136/9/435
weights (<i>a</i> , <i>b</i>) ^b	0.02, 0	0.05, 0.4
GOF <i>S</i> (<i>F</i> ²) ^c	1.616	1.022
<i>R</i> 1(<i>F</i>), <i>I</i> > 2σ(<i>I</i>) ^d	0.0381	0.0344
w <i>R</i> 2(<i>F</i> ²), all data ^e	0.0870	0.0937
largest diff peak, hole (e Å ⁻³)	0.237, –0.201	0.230, –0.257

^a $R_{\text{int}} = \frac{\sum |F_o^2 - F_{\text{mean}}^2|}{\sum |F_o^2|}$; $R_{\sigma} = \frac{\sum |\sigma(F_o^2)|}{\sum |F_o^2|}$. ^b $w = 1/[\sigma^2(F_o^2) + (aP)^2 + bP]$, where $P = (F_o^2 + 2F_c^2)/3$. ^c $S = [\sum w(F_o^2 - F_c^2)^2 / (n - p)]^{1/2}$, where n is the number of reflections and p is the number of refined parameters. ^d $R1(F) = \frac{\sum ||F_o| - |F_c||}{\sum |F_o|}$. ^e $wR2(F^2) = [\sum w(F_o^2 - F_c^2)^2 / \sum wF_o^4]^{1/2}$.

Some of the hydrogen atoms were clearly found in a difference Fourier maps (in particular hydrogen atoms involved in hydrogen

bonding); however, they were eventually placed in idealized position and refined riding on their parent atom with an isotropic displacement parameter of 1.2 (1.5 for the hydroxo group) times that of the pertinent parent atom.

The structure of **4**·1/2CH₂Cl₂ suffers from a disorder of the dichloromethane solvate molecule. Because it was difficult to refine a consistent disordered model (possibly because of the large volume, 200 Å³, of the cavity occupied by the solvent), its contribution was subtracted from the observed structure factor according to the BYPASS procedure,²⁹ as implemented in PLATON.³⁰

The 7-azaindolum cation in **5** is disordered over two orientations, in which the five- and six-member rings are exchanged. It was possible to resolve the two individuals, whose refined partial occupation factors are 0.647(6) and 0.353(6). Bond distances in the two disordered components were restrained to be equal within a tolerance of 0.01 Å. The nitrogen atoms were unambiguously identified on the basis of their position and their proximity to suitable hydrogen-bond acceptors.

The final difference electron density map showed no features of chemical significance, with the largest peaks lying close to the fluorine atoms of the pentafluorophenyl substituents. Final conventional agreement indices and other structure refinement parameters are listed in Table 8.

Acknowledgment. T.B. thanks Prof. Angelo Gavezzotti for helpful discussion. Thanks are due to the Italian CNR (ISTM) for providing facilities for inert-atmosphere and low-temperature experiments.

Supporting Information Available: Twelve figures showing details of the NMR experiments. This material is available free of charge via the Internet at <http://pubs.acs.org>. CCDC 279502 and 279503 contain the supplementary crystallographic data for this paper. These data can be obtained free of charge via <http://www.ccdc.cam.ac.uk/conts/retrieving.html> (or from the CCDC, 12 Union Road, Cambridge CB2 1EZ, UK; fax: +44–1223–336033; e-mail: deposit@ccdc.cam.ac.uk).

IC051285P

(29) van der Sluis, P.; Spek, A. L. *Acta Crystallogr., Sect. A* **1990**, *46*, 194.

(30) Spek, A. L. *J. Appl. Crystallogr.* **2003**, *36*, 7.

(31) Allen, F. H.; Kennard, O.; Watson, D. G.; Brammer, L.; Orpen, A. G.; Taylor, R. *J. Chem. Soc., Perkin Trans. 2* **1987**, S1.